J Mater Sci (2011) 46:6243–6247
DOI 10.1007/s10853-011-5557-x

ABBASCHIAN FESTSCHRIFT

Measurement of surface tension and specific heat of Ni-18.8 at.% Si alloy melt by containerless processing

Chongde Cao · Limin Zhang · Xiaojun Bai · Libing Duan · Fang Wang

Received: 31 October 2010 / Accepted: 9 April 2011 / Published online: 21 April 2011

Abstract The surface tension and specific heat of superheated and undercooled Ni-18.8 at.% Si alloy melt have been measured by the oscillating drop method and the drop calorimetry technique in combination with electromagnetic levitation, respectively. The surface tension follows a linear relationship with temperature within the range of 1370–2100 K. The surface tension at the melting temperature and the temperature coefficient are determined to be 1.796 N/m and -3.858×10^{-4} N/m/K, respectively. The specific heat is determined to be 40.80 ± 1.435 J/mol/K over the temperature range 1296–2000 K. The maximum undercooling of 178 K is achieved in the experiments. Based on the measured data of surface tension and specific heat, the viscosity, solute diffusion coefficient, density and thermal diffusivity of liquid Ni-18.8 at.% Si alloy are calculated.

Introduction

Reliable thermophysical properties data of liquid metals and alloys, such as surface tension, specific heat, viscosity, diffusion coefficient and so on, are of great significance for liquid physics, solidification theoretical models, and computational materials science, which have aroused great research interest in the past decades [1–4]. Many techniques and methods have been developed to determine the thermophysical parameters of a liquid metal or alloy above its melting point. In contrast, only a little information is available on experimental studies of thermophysical properties of highly undercooled liquid alloys because an undercooled liquid is in the metastable state and therefore, it is difficult to measure the parameters with conventional methods [5]. In particular, such data for high-temperature metallic alloys are scarce. This restricts better understanding of rapid solidification, metastable phase transformation, and metastable phase diagram. It is well known that surface tension and specific heat are the most important for crystal nucleation and growth, glass-forming ability of bulk melts, solidification thermodynamics and kinetics [6–8].

So far, several experimental methods, such as maximum bubble pressure method [9], sessile drop method [10], pendant drop method [11], and oscillating drop method [12], have been developed to measure the surface tension of liquids. For liquid metals, electromagnetic levitation provides containerless processing capabilities and, therefore, liquid metals can be easily undercooled. The oscillating drop technique using electromagnetic levitation has proven to allow precise determination of surface tension of an undercooled liquid metal or alloy [13–16]. If the specific heat of liquid metals or alloys is determined accurately, some other parameters like the Gibbs free energy difference, the entropy difference, and the enthalpy difference between the melt and the crystal can be deduced [17]. These are more favorable to further studies on modeling nucleation and growth kinetics. There are two main experimental methods to investigate the specific heat of undercooled liquid metals or alloys, namely differential scanning calorimetry (DSC) and drop (DC) calorimetry techniques. The former is only suitable to some metals or alloys with low melting point, where heterogeneous

C. Cao (✉) · L. Zhang · X. Bai · L. Duan
Department of Applied Physics, Northwestern Polytechnical University, Xian 710072, China
e-mail: caocd@nwpu.edu.cn

F. Wang
School of Computer Science and Technology, Northwestern Polytechnical University, Xian 710072, China

nucleation from the container wall cannot be avoided. For high melting point metals and alloys, the latter method is more applicable, which provides a containerless processing environment to avoid contamination and to achieve high undercooling [18].

In this study, the surface tension and specific heat of Ni-18.8 at.% Si alloy melt have been measured by the oscillating drop method and drop calorimetry method using electromagnetic levitation, respectively. Some other thermophysical properties, such as the viscosity, solute diffusion coefficient, density and thermal diffusivity, were further derived on the basis of the experimental data of surface tension and specific heat.

Experimental

The alloy samples with a mass of 0.6–0.7 g were prepared from pure nickel (99.998%) and Si (99.9999%) in an arc-melting furnace under 99.999% argon atmosphere. The chamber was evacuated to better than 10^{-5} Pa and then backfilled with argon and helium with a volume ratio of 1:1. The sample was levitated and melted by RF inductive heating and then cooled by He-22 vol.% H_2 flowing through liquid nitrogen. An infrared pyrometer was used for temperature monitoring. When the alloy melt was undercooled to an expected temperature, the gas flow rate was adjusted to keep the melt at this temperature for enough time for signal acquisition. During levitation the surface tension caused oscillation of the drop surface. In order to eliminate the influence of induction, the oscillation signals detected by a photodiode passed through a low-pass filter with a frequency threshold of 110 Hz, an amplifier and an A/D converter, and were recorded by a computer. The Fast Fourier Transformation (FFT) transformation was then performed off-line to obtain the oscillation frequency. Finally, the sample dropped into the adiabatic calorimeter after the induction power was switched off. The temperature rise of the calorimeter was measured for enthalpy change calculation and the temperature of the calorimeter shell was adjusted by a Eurotherm 818P temperature controller/programmer.

Results and discussion

Surface tension

The surface tension measurement principle using the levitated drop technique is based on Rayleigh equation [19]. Cummings and Blackburn [20] derived the frequency sum rule to obtain the Rayleigh frequency considering the influence of a magnetic field on the split modes under the terrestrial levitation conditions. Detailed description of the theoretical background can be found in Refs. [12, 18, 21]. In this study, the levitated droplet is always rotated and thus the Rayleigh frequency splits into five peaks.

Figure 1 shows the measured surface tension of Ni-18.8 at.% Si alloy melt over a temperature range of 1370–2100 K. The maximum undercooling attains 127 K. The surface tension shows a well linear relationship with temperature:

$$\sigma = (1.796 \pm 0.0027) - (3.858 \pm 0.085) \times 10^{-4}(T - T_{\mathrm{L}})\,\mathrm{N/m} \tag{1}$$

where T_{L} is the liquidus temperature, 1474 K, of Ni-18.8 at.% Si alloy. With the increase of temperature the surface tension of Ni-18.8 at.% Si alloy melt decreases in the experimental temperature range.

The measured data of surface tension of pure liquid Ni [12], pure liquid Si [13], and other Ni-Si alloys containing 9.9 at.% [22] and 29.8 at.% Si [23] are also illustrated in Fig. 1 for comparison. The surface tension of liquid Ni, Si, and the Ni–Si alloys shows descending tendencies with the increase of temperature. The surface tension and its temperature coefficient of liquid silicon are smaller than those of liquid nickel. Both the surface tension at liquidus temperature and the temperature coefficient of Ni-18.8 at.% Si alloy set intermediate values in comparison with those of pure nickel and silicon. However, the surface tension of Ni-18.8 at.% Si alloy is larger than those of Ni-9.9 at.% Si and Ni-29.8 at.% Si alloys. The scattering triangles and squares represent the measured surface tension of Ni-29.8, 18.8 and 9.9 at.% Si alloys at 1773 K [24] and 1823 K [25], respectively. The positions of different compositions are indicated by an arrow. For all these alloys, the surface tension and temperature coefficient measured by drop calorimetry technique are

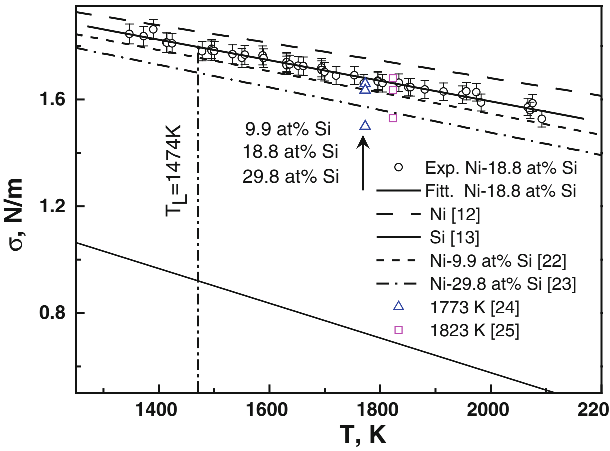

Fig. 1 Measured surface tension of liquid Ni, Si, and Ni-Si alloys as functions of temperature: *open circle* Ni-18.8 at.% Si in this study; measured surface tension at 1773 K (*open triangle*) [24] and 1823 K (*open square*) [25] for Ni-29.8, 18.8, and 9.9 at.% Si alloys as indicated by an *arrow*

larger than those measured by maximum bubble pressure method [24–26]. According to previous study [24–26], both surface tension and temperature coefficient of Ni-Si alloys decreases with the increase of Si concentration. The low values are possibly related to contamination with low concentrations of oxygen or other surface active elements [26].

Specific heat

The specific heat can be described as the differential coefficient of enthalpy change ΔH with respect to temperature T in the experimental temperature range. At a certain temperature, the levitated alloy melt sphere drops into the adiabatic calorimeter. The temperature change of the adiabatic calorimeter can be determined accurately. On the basis of energy conservation principle, the enthalpy change of the sample can be determined by [17]

$$\Delta H = H(T) - H(293) = \frac{M}{m} C_{\mathrm{PS}}^{\mathrm{Cu}}(T_{\mathrm{e}} - T_0) + C_{\mathrm{PS}}^{293}(T_{\mathrm{e}} - 293) + \frac{Q_{\mathrm{lost}}}{m} \quad (2)$$

where $H(T)$ is the enthalpy of the sample at temperature T, $H(293)$ the enthalpy at the reference temperature (293 K), M and m the mass of the calorimeter block and the sample, respectively, $C_{\mathrm{PS}}^{\mathrm{Cu}}$ is the specific heat of the calorimeter block which is calibrated as 24.53 J/mol/K, C_{PS}^{293} is the specific heat of the sample at 293 K, T_0 and T_{e} are the initial temperature and equilibrium temperature of the calorimeter, respectively, and Q_{lost} is the heat of system lost to the environment, which is expressed by

$$Q_{\mathrm{lost}} = A\varepsilon_{\mathrm{H}}\sigma_{\mathrm{SB}}(T^4 - T_0^4)t_{\mathrm{D}} + S(T - T_0)\int_0^{t_{\mathrm{D}}} \alpha_{\mathrm{C}}\,\mathrm{d}t \quad (3)$$

where the first item is related to heat radiation and the second to convection. S is the surface area of the sample, ε_{H} is the emissivity, σ_{SB} the Stafan-Boltzmann constant, and t_{D} the dropping time. α_{C} is the heat transfer coefficient of the inert gas:

$$\alpha_{\mathrm{c}} = \frac{\lambda_{\mathrm{g}}}{d}\left[2 + 0.6(v_{\mathrm{r}} d\rho_{\mathrm{g}}/\eta_{\mathrm{g}})^{1/2}(c_{\mathrm{g}}\eta_{\mathrm{g}}/\lambda_{\mathrm{g}})^{1/3}\right] \quad (4)$$

here λ_{g}, ρ_{g}, η_{g}, and c_{g} are the thermal conductivity, density, viscosity, and specific heat of the ambient gas, respectively. V_{r} is the relative dropping speed with ambient gas. d is the diameter of the levitated droplet.

Since the enthalpy change of the sample is determined by Eq. 2, the specific heat, C_{PL}, can be derived by

$$C_{\mathrm{PL}} = \frac{\partial[H(T) - H(293)]}{\partial T} \quad (5)$$

The measured data and parameters on the enthalpy of liquid Ni-18.8 at.% Si alloy are listed in Table 1. The thermophysical parameters of Ar, He, and H_2 at different temperatures used for calculation are listed in Table 2. Figure 2 presents the enthalpy of Ni-18.8 at.% Si alloy melt within the temperature range of 1300–2000 K, where the maximum undercooling and superheating attain 178 and 526 K, respectively. It can be found that the enthalpy change of Ni-18.8 at.% Si alloy linearly increases with the increase of temperature:

$$H(T) - H(293) = -(8.825 \pm 2.148) \times 10^3 + (40.80 \pm 1.435)T\,\mathrm{J/mol} \quad (6)$$

Accordingly, the average specific heat of Ni-18.8 at.% Si alloy melt in the temperature range of 1300–2000 K can be determined to be 40.80 ± 1.435 J/mol/K. This value is lower than the specific heat of pure liquid Ni [27] and larger than that of Ni-29.8 at.% Si alloy [23].

Related thermophysical properties

The important physical parameters of liquid alloys, viscosity, solute diffusion coefficient, and density are intensively correlative to mass transport during solidification. Such parameters are especially scarce for undercooled alloy melts because it is extremely difficult to measure them due to the metastable state under high undercooling conditions. Fortunately, these parameters can be calculated from surface tension with some empirical models [28–30], which are given by

$$\eta = \frac{16}{15}\sqrt{\frac{M_{\mathrm{a}}}{kT}} \cdot \sigma \quad (7)$$

Table 1 The parameters and measured enthalpy differences of Ni-18.8 at.% Si alloy melt

T (K)	A (cm^2)	m (g)	$T_0 - T_{\mathrm{e}}$ (K)	T_{e} (K)	Q_{lost} (J/mol)	ΔH (J/mol)
1438	0.9776	0.596	1.0681	292.9119	4.88	48437.0
1414	0.9805	0.601	1.1000	296.5281	4.69	49485.6
1638	1.0082	0.600	1.2563	298.2093	6.75	56813.9
1998	1.0846	0.621	1.6844	297.4594	11.94	73815.1
1379	0.9887	0.613	1.0672	306.0302	4.43	47330.3
1617	1.0058	0.600	1.2594	306.4314	6.50	57095.9
1329	1.1805	0.808	1.3484	301.4234	4.65	45234.1
1331	1.1910	0.818	1.3625	304.534	4.68	45201.4
1500	1.2728	0.875	1.6563	303.4688	6.48	51366.6
1313	1.1738	0.803	1.2969	303.3284	4.50	43802.6
1770	1.0341	0.607	1.4031	306.3437	8.32	63013.2
1296	0.9653	0.601	1.0275	303.1025	3.81	46391.3
1399	1.2869	0.907	1.6050	302.3963	5.55	47958.7
1338	1.2120	0.839	1.4437	301.9575	4.81	46635.2

Table 2 Thermophysical parameters of Ar, He, and H_2 at different temperatures

T (K)	Gas	λ_g (J/m/s/K)	ρ_g (g/cm^3)	η_g(g/m/s)	C_g (J/g/K)
1200	Ar	0.0489	0.000401	0.059	0.52
	He	0.45	0.0000401	0.0508	5.19
	H_2	0.528	0.00002004	2.262×10^{-5}	15.5
1500	Ar	0.056	0.000320	0.0684	0.52
	He	0.479	0.000032	0.0586	5.19
	H_2	0.655	0.00001603	2.616×10^{-5}	16.15
1800	Ar	0.0626	0.000266	0.076	0.52
	He	0.543	0.0000267	0.0657	5.19
	H_2	0.786	0.00001336	2.961×10^{-5}	16.8

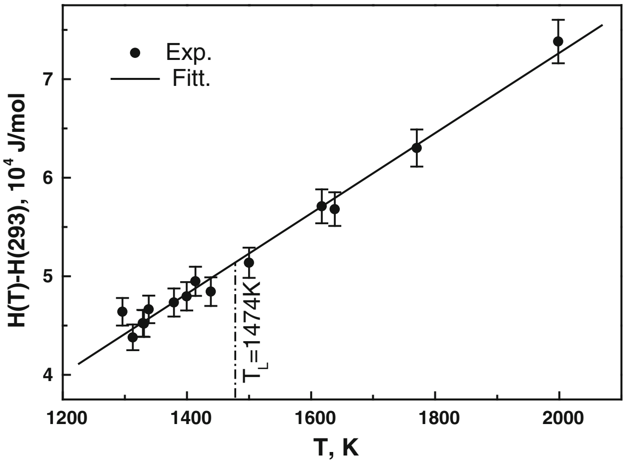

Fig. 2 Measured enthalpy change of Ni-18.8 at.% Si alloy melts as a function of temperature

$$D = \frac{5kT}{32\pi r\sigma}\sqrt{\frac{kT}{M_a}} \tag{8}$$

$$\sigma\left(\frac{M_r}{\rho}\right)^{\frac{2}{3}} = K_c(T_c - T) \tag{9}$$

where η, D, and ρ are viscosity, solute diffusion coefficient, and density, respectively. M_a is the absolute atomic mass, M_r the relative atomic mass, k the Boltzmann constant; K_c a constant equal to 6.4×10^{-8} J/K for liquid metals [29], T_c is the critical temperature at which the liquid–gas interface disappears and r the characteristic radius of solute atom. For Ni-18.8 at.% Si alloy melt, r is the radius of Si atom, and T_c can be derived from Eq. 9 at the melting point.

Figure 3 illustrates the data of calculated viscosity, solute diffusion coefficient, and density of Ni-18.8 at.% Si alloy melt depending on temperature. In order to get the activation energies for viscosity and solute diffusion, the temperature dependence of viscosity and solute diffusion coefficient can also be fitted by an exponential law, as presented in Eqs. 10 and 11.

$$\eta = 1.486\exp(1.2062 \times 10^4/RT)\ \text{mPa s} \tag{10}$$

$$D = 1.689 \times 10^{-8}\exp(-2.7226 \times 10^4/RT)\ \text{m}^2/\text{s} \tag{11}$$

where R is the gas constant, 8.314 J/mol/K. From Eqs. 10 and 11, the activation energies for viscosity and solute diffusion are derived to be 12.062 and 27.226 kJ/mol, respectively. With the increase of temperature, the density of Ni-18.8 at.% Si alloy melt decreases linearly:

$$\rho = 6.511 - 1.272 \times 10^{-3}(T - T_L)\ \text{g/cm}^3 \tag{12}$$

The most important parameters for heat transfer in a liquid metal or alloy, thermal diffusivity, κ, and thermal conductivity, λ, are related to density and specific heat (Eq. 13).

$$\kappa = \lambda/(\rho C_{PL}) \tag{13}$$

According to the well-known Wiedemann–Franz–Lorenz law [31], the product of the thermal conductivity and electrical resistivity is the same for all metals:

$$\frac{\lambda\rho_e}{T} = \frac{\pi^2k^2}{3e^2} \tag{14}$$

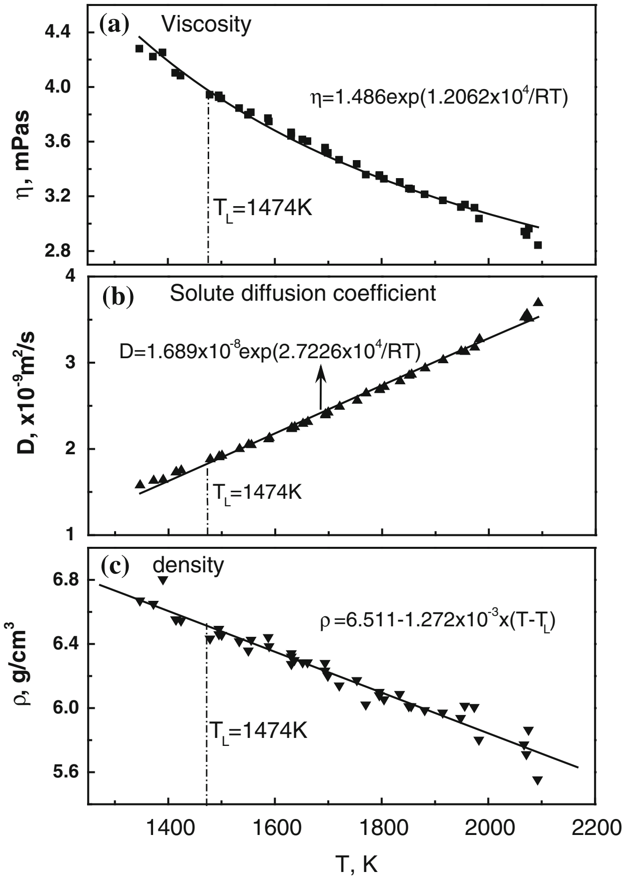

Fig. 3 Calculated viscosity (**a**), solute diffusion coefficient (**b**), and density (**c**) of Ni-18.8 at.% Si alloy melt as functions of temperature

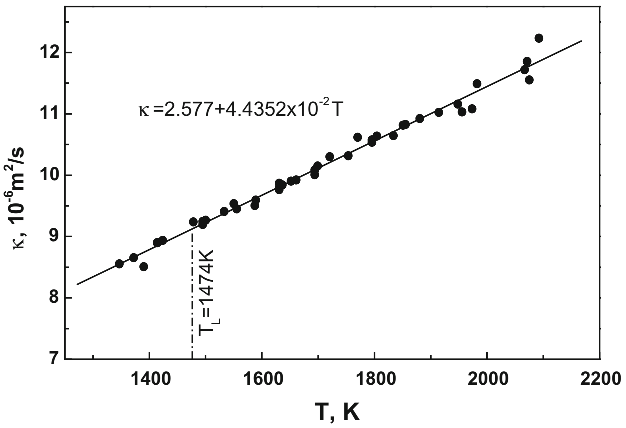

Fig. 4 Calculated thermal diffusivity of liquid Ni-18.8 at.% Si alloy as a function of temperature

where ρ_e is the electrical resistivity, and e represents the basic electron charge.

On the basis of the electrical resistivity of pure liquid Ni and Si, the electrical resistivity of Ni-18.8 at.% Si alloy can be estimated according to Neumann–Kopp rule [13], i.e., $\rho_e = 0.0307T + 33.79$ μΩ cm. Thus, the thermal diffusivity can be obtained to be $\kappa = 2.577 \times 10^{-6} + 4.4352 \times 10^{-9}T$ m^2/s, as shown in Fig. 4.

Conclusions

The oscillating drop method and drop calorimetry technique in combination with electromagnetic levitation were employed to measure the surface tension and specific heat of superheated and undercooled liquid Ni-18.8 at.% Si alloy. The surface tension of liquid Ni-18.8 at.% Si alloy has been determined as $\sigma = (1.796 \pm 0.0027) - (3.858 \pm 0.085) \times 10^{-4}(T - T_L)$ N/m over a temperature range 1370–2100 K. The enthalpy change was measured and the average specific heat of this alloy was determined to be 40.80 ± 1.435 J/mol/K in the temperature range of 1296–2000 K, where the corresponding maximum undercooling attains 178 K. The viscosity, solute diffusion coefficient, density, and thermal diffusivity of this alloy in the liquid state have also been calculated on the basis of the measured data of surface tension and specific heat. The activation energies for viscosity and solute diffusion have been estimated from the data of viscosity and solute diffusion coefficient depending on temperature. The density and thermal diffusivity exhibit linear relationships with temperature.

Acknowledgements This study was supported by the National Natural Science Foundation of China (Grant No. 50871088), NPU-FFR, Fundamental Research Foundation of Shaanxi and the Foundation of Key Laboratory for Liquid–Solid Structural Evolution and Processing of Materials, Ministry of Education, Shandong University, P.R. China.

References

1. Keene B (1988) Int Mater Rev 33:1
2. Keene B (1993) Int Mater Rev 38:157
3. Mills K, Su Y (2006) Int Mater Rev 51:329
4. Egry I, Brillo J, Matsushita T (2005) Mater Sci Eng A 413–414:460
5. Egry I, Brillo J (2009) J Chem Eng Data 54:2347
6. Chan WL, Averback RS, Cahill DG (2009) Phys Rev Lett 102:095701
7. Plevachuk Y, Hoyer W, Kaban I, Kohler M, Novakovic R (2010) J Mater Sci 45:2051. doi:10.1007/s10853-009-4120-5
8. Su YC, Mills K, Dinsdale A (2005) J Mater Sci 40:2185. doi:10.1007/s10853-005-1930-y
9. Goicoechea J, Garcia-Cordovilla C, Louis E, Pamies A (1991) Scripta Metall Mater 25:479
10. Li Z, Mills KC, McLean M, Mukai K (2005) Metall Mater Trans B 36:247
11. Roe RJ, Bacchetta VL, Wong PMG (1967) J Phys Chem 71:4190
12. Egry I, Lohoefer G, Jacobs G (1995) Phys Rev Lett 75:4043
13. Przyborowski M, Hibiya T, Eguchi M, Egry I (1995) J Cryst Growth 151:60
14. Wang HP, Yao WJ, Cao CD, Wei B (2004) Appl Phys Lett 85:3414
15. Li JQ, Ishikawa T, Okada JT, Watanabe Y, Yu JD, Yoda S, Yuan ZF (2009) J Mater Res 24:2449
16. Egry I, Holland-Moritz D, Novakovic R, Ricci E, Wunderlich R, Sobczak N (2010) Int J Thermophys 31:949
17. Wang N, Han XJ, Wei B (2002) Appl Phys Lett 80:28
18. Wang HP, Cao CD, Wei B (2004) Appl Phys Lett 84:4062
19. Rayleigh L (1879) Proc R Soc Lond 29:71
20. Cummings DL, Blackburn DA (1991) J Fluid Mech 224:395
21. Fujii H, Matsumoto T, Nogi K (2000) Acta Mater 48:2933
22. Wang HP, Chang J, Wei B (2009) J Appl Phys 106:033506
23. Wang HP, Wei B (2005) Chin Sci Bull 50:945
24. Vasiliu MI, Eremenko VN (1965) Poroshkovaya Metall 3:80
25. Shergin LM, Popel SI, Tsarevskii BV (1971) AN SSSR Ural'sk Nauchn Tsentr Trudy Inst Metall 25:52
26. Keene BJ (1987) Surf Interface Anal 10:367
27. Egry I (1993) Scr Metall Mater 28:1273
28. Schaefers K, Rosner-Kuhn M, Frohberg MG (1995) Mater Sci Eng A 197:83
29. Smithlls CJ (1984) Metals reference book, 6th edn. Butterworth, London
30. Eötvös R, Wieldeman S (1886) Ann Phys 27:448
31. Iida T, Guthrie RIL (1993) The physical properties of liquid metals, vol 134. Oxford Science Publications, Claredon, Oxford